Available online at www.sciencedirect.com
SCIENCE DIRECT®
Journal of Power Sources 129 (2004) 330–342
JOURNAL OF POWER SOURCES
www.elsevier.com/locate/jpowsour

Microcontroller-based on-line state-of-charge estimator for sealed lead–acid batteries

Y. Çadırcı [a,b,*], Y. Özkazanç [a]

[a] *Electrical and Electronics Engineering Department, Hacettepe University, Beytepe Campus, TR06532 Ankara, Turkey*
[b] *SİSTAŞ Digital Telecommunication Industries, TR06640 Küçükesat, Ankara, Turkey*

Received 5 May 2003; received in revised form 28 October 2003; accepted 3 November 2003

Abstract

This paper presents a microcontroller-based, on-line battery state-of-charge (SOC) estimator, and monitoring system for sealed lead–acid batteries, used as back-up power supplies in various applications. The proposed SOC estimation system consists of a combination of the discharge time versus discharge rate data given in manufacturers' data sheets, and coulometric measurements. Battery SOC monitoring tests have been carried out under both constant and dynamic load conditions, and for alternate charge–discharge cycles of lead–acid batteries of different capacities, and for different operating temperatures. The test results have shown that a very good accuracy in the estimation of available capacity is obtained for various practical operating conditions. Changes in battery characteristics which occur due to ageing are also taken into account by estimating the actual capacity of the battery, and adopting the corresponding recharacterization of the aged lead–acid cells.

Keywords: Sealed lead–acid batteries; Available capacity; State-of-charge; Capacity estimation

1. Introduction

The energy capability of a battery depends on both constructional parameters such as material composition and geometry, and operating parameters such as the discharge rate (load current), temperature, age, and end voltage. The available charge, or state-of-charge (SOC) of the battery is a complex function of these parameters, as well as the service history. A continuous, on-line indication of SOC of batteries, and estimation of their available capacity are of considerable importance for continuity of service. Several practical techniques are available to estimate SOC of lead–acid batteries [1–10] such as specific gravity, open-circuit voltage, loaded voltage, and coulometric measurements (ampere-hour counting). Monitoring of SOC by the use of wire wound coils with an accuracy of ±10%, and the optical absorption techniques have also been described in the literature [11,12].

The specific gravity is a direct indication of the SOC because, it shows the concentration of acid in the electrolyte. The measurement is performed with a hydrometer, but it is impractical for continuous use due to lengthy stabilization period required after charge or discharge cycles. The open-circuit voltage measurement is also an accurate indicator of SOC but, similar to the specific gravity measurements, it requires quite a long stabilization period. Hence, this method cannot provide a continuous, on-line indication of the SOC, as required in applications where the continuity of service is of utmost importance.

For a constant load current, which is not the case for most equipment, loaded voltage measurements also can give an indication of the remaining capacity of lead–acid cells. Various models have been proposed based on the discharge voltage versus time characteristics. Estimates of SOC have been made by redrawing manufacturer's discharge voltage versus time characteristics based on changes in internal battery parameters [2] to be measured. Some curve fitting models have been employed to match the discharge voltage versus time characteristics to exponential, parabolic, and hyperbolic curves [3–5]. A parameter set is then required for each discharge condition, besides the necessity for accurate voltage measurements over a narrow range. Evaluation of lead–acid battery capacity using a mathematical model taking into account self-discharge, battery storage capacity, internal resistance, and environmental temperature has been presented in [6]. The relationship between discharge voltage and SOC,

* Corresponding author. Present address: SİSTAŞ Digital Telecommunication Industries, TR06640 Küçükesat, Ankara, Turkey. Tel./fax: +90-312-4171552.
E-mail address: sistas@sistas.com.tr (Y. Çadırcı).

0378-7753/$ – see front matter © 2003 Elsevier B.V. All rights reserved.
doi:10.1016/j.jpowsour.2003.11.008

valid for a wide range of discharge rates, and temperatures has been employed in [7] as related to telecommunications back-up power supply application, with an estimation accuracy of not less than 10%, after 10% discharge of rated capacity.

In coulometric measurements, however, the amount of capacity taken out or put into a battery are measured in terms of ampere-hour. Charge accumulation techniques [8], where SOC is determined by monitoring battery charge and discharge current are impractical in the long term due to accumulation of error. The use of correction factors is required when different discharge rates and ambient temperatures are employed. These are only average estimated values, and do not cover all combinations of operating conditions. A monitoring technique combining the open-circuit voltage under no-load condition, and coulometric measurements under constant load has been implemented in [9] on a microcomputer-based circuit. In this technique, a 30 min rest period was used in measuring the open-circuit voltage. Each of these techniques has its own drawbacks. Some of them require the measurement of open-circuit battery voltage over relatively long time periods, which is not practical in applications where batteries should always remain connected to the system as back-up, for continuity of service. Furthermore, SOC monitoring based on battery voltage measurement under load requires a high resolution, in order to obtain accurate results of estimation in the flat portion of the non-linear discharge characteristics.

In this paper, a microcontroller-based, on-line SOC estimator has been proposed for sealed lead–acid batteries during both discharge, and charge periods, using a combination of the actual battery discharge time versus discharge rate data, and coulometric measurements. The proposed technique does not require any open-circuit battery voltage measurement. The available capacity of the battery is estimated automatically at the end of each discharge period by measuring the battery voltage, and at the end of each charge period by measuring the battery current. The proposed system has been implemented to monitor the SOC of sealed lead–acid battery blocks used as telecommunication back-up power supplies, and tested in the field under various operating conditions.

2. SOC estimation

Discharge time against discharge rate data of lead–acid batteries given in manufacturers' data sheets are used to take into account the effect of discharge current rate during coulometric measurements. The coefficients of discharge current rate thus obtained are then combined with battery current, and ambient temperature measurements for on-line monitoring of the battery SOC, during discharge periods. During charge, only coulometric measurements are made by taking into account the charging efficiency, and ambient temperature, for either constant voltage or constant-current charge strategies.

2.1. SOC estimation during discharge

The curves in Fig. 1 illustrate the typical discharge characteristics of sealed lead–acid batteries for an ambient temperature of 20 °C [1]. '*C*' expresses the available capacity of the battery measured at 20 h discharge rate. Available capacity of a maintenance-free sealed lead–acid battery is determined at 20 °C, by discharging the battery at a 20 h rate to an end voltage of 1.75 V per cell. The dotted line in Fig. 1 indicates the lowest recommended voltage (end voltage) under load, at various discharge rates. In general, lead–acid batteries are damaged in terms of capacity, and service life if discharged below these recommended end voltages.

Actual capacity of the battery is different from the available capacity when it is discharged at a rate higher than 20 h discharge rate. It is clear from Fig. 1 that the ampere-hour

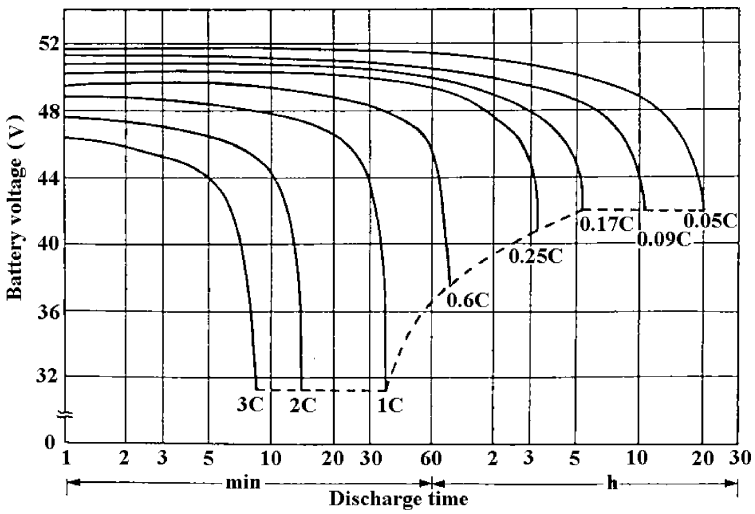

Fig. 1. Typical discharge curves of a 4 × 12 V lead–acid battery block at various discharge rates ($T = 20\,^{\circ}C$).

capacity of the battery decreases with increasing discharge current rate, e.g. for $0.05C$ discharge rate, ampere-hour capacity is $0.05C \times 20 = 1C$, but for $0.17C$ discharge rate, ampere-hour capacity reduces to $0.17C \times 5.5 = 0.935C$. Therefore, during discharge period, it is not possible to estimate the battery SOC only by accumulating the ampere-hour capacity, but some modifications should be made. In the proposed estimation method, the used capacity, $C_u(t)$, is defined as:

$$C_u(t) = \int_0^t k(A)A\,dt \tag{1}$$

where A is the discharge current rate, and $k(A)$ the coefficient for discharge current rate.

Moreover, the capacity of 20 h discharge is defined as the available battery capacity, and is expressed as:

$$C = A_{20} \times 20 \tag{2}$$

where C is the available capacity, and A_{20} the discharge current rate for 20 h discharge.

The keypoint in estimating SOC during discharge period is to calculate the coefficient for discharge current rate, $k(A)$. The factor $k(A)$ can be calculated by using the manufacturers' data sheets. In these data sheets, tables are given to indicate the necessary time to discharge a battery down to 1.75 V per cell level, for different constant discharge current levels. From Eq. (1):

$$C' = \int_0^{t_{di}} k(A_i)A_i\,dt \tag{3}$$

where C' is the capacity, t_{di} the necessary time duration to discharge the battery to 1.75 V per cell corresponding to A_i given in data sheets, A_i the constant discharge current given in manufacturer's data sheet, and $k(A_i)$ the coefficient for A_i.

As A_i is constant for a given discharge current, Eq. (3) becomes:

$$C' = k(A_i)A_i t_{di}$$

$$\Rightarrow k(A_i) = \frac{C'}{A_i t_{di}} \tag{4}$$

However, there is a critical point, which should be taken into account while using the manufacturers' data sheets for SOC estimation during discharge. As it is already stated, tables in these data sheets give the necessary time to discharge a battery down to a constant voltage level, i.e. 1.75 V per cell, for different constant discharge currents. As it is seen from Fig. 1, the higher the discharge current, the lower the end voltage of the battery. Therefore, the available capacity of the battery can be formulated as given in (5).

$$C = \int_0^{t_{di}} k(A_i)A_i\,dt + \int_{t_{di}}^{t_{ev}} k(A_i)A_i\,dt \tag{5}$$

$$\Rightarrow C = C' + \int_{t_{di}}^{t_{ev}} k(A_i)A_i\,dt \tag{6}$$

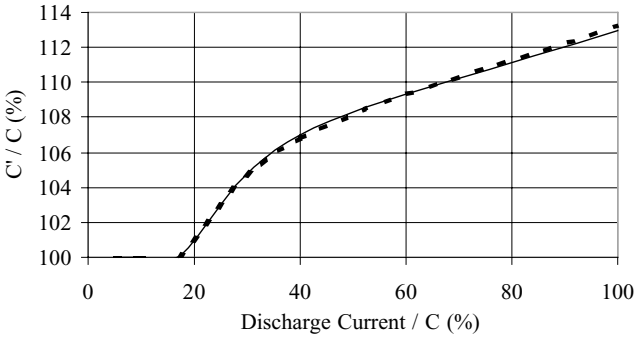

Fig. 2. C'/C vs. normalized discharge current.

where t_{ev} is the necessary time duration to discharge the battery to the end voltage.

By using Fig. 1, C from Eq. (6) and C' from Eq. (3) are calculated for different discharge current levels, and C/C' versus normalized discharge current characteristic is plotted in Fig. 2. Various manufacturers' data are examined, and it is concluded that the relationship between C and C' can be generalized within ±1% error. The equation of the curve in Fig. 2 is found out by curve fitting method, and is used when discharge current exceeds $0.17C$. C/C' is denoted as $k_{ev}(A_i)$, and is calculated from Eq. (7).

$$k_{ev}(A_i) = \frac{C}{C'} = \begin{cases} 1 & \text{for } p \le 17 \\ \dfrac{5.05\ln(p-16)+100}{100} & \text{for } p > 17 \end{cases} \tag{7}$$

where $p = (A_i/C)100$

From Eq. (7),

$$C' = \frac{C}{k_{ev}(A_i)} \tag{8}$$

Therefore, by replacing C' into (4), Eq. (9) is obtained.

$$k(A_i) = \frac{C}{k_{ev}(A_i)A_i t_{di}} = \frac{A_{20} \times 20}{k_{ev}(A_i)A_i t_{di}} \tag{9}$$

k_{dc} is defined as:

$$k_{dc}(A_i) = \frac{C}{A_i t_{di}} = \frac{A_{20} \times 20}{A_i t_{di}} \tag{10}$$

Then,

$$k(A_i) = \frac{k_{dc}(A_i)}{k_{ev}(A_i)} \tag{11}$$

In Appendix A, $k_{dc}(A_i)$ versus normalized A_i curves are given for different lead–acid batteries. It can be observed that, even for different battery types from the same manufacturer the deviation between these battery curves increases with increasing current, and it reaches ≈10%. It can therefore be concluded that it is not suitable to use a single curve for all kinds of batteries. It is necessary to obtain the curves of $k_{dc}(A_i)$ versus normalized A_i during discharge, for each battery type by using the manufacturers' data.

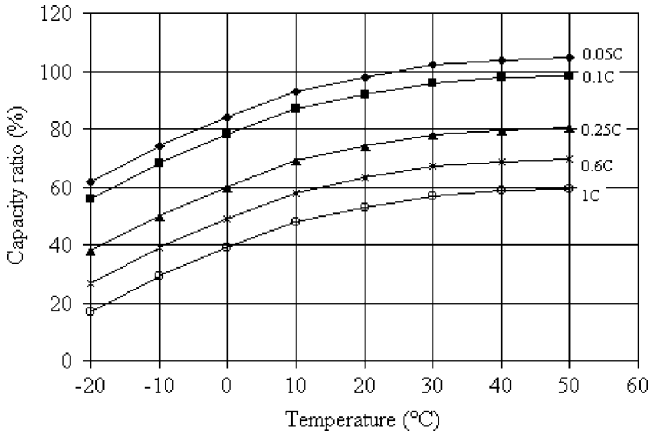

Fig. 3. Capacity ratio vs. ambient temperature as a function of discharge capacity.

The capacity of sealed lead–acid cell, as with most batteries, is not only dependent on the discharge rate, but also the temperature. As temperature rises, the electrochemical activity in the battery increases, hence electrical capacity that can be taken out of it increases. Fig. 3 shows the relation between temperature and discharge capacity as a ratio of available capacity. Since the capacity ratio versus temperature curves are all in parallel, a single curve can be used to take into account the effect of temperature in addition to that of discharge current taken into account by the coefficient $k(A_i)$ defined above. For this purpose, the curve corresponding to $0.05C$ from Fig. 4 is chosen, and the equation of the curve is found out by curve fitting method. Hence, the relationship between the capacity in percent and temperature (T) is given by

$$\text{capacity ratio (\%)} = -0.0102T^2 + 0.9082T + 84.137 \quad (12)$$

In order to take into account the effect of temperature in SOC estimation, another coefficient which is denoted by $k_T(T)$ is calculated, and Eq. (1) is modified as:

$$C_u(t) = \int_0^t k_T(T)k(A)A\,dt \quad (13)$$

$$\text{where } k_T(T) = \frac{1}{\text{capacity ratio (\%)}} \quad (14)$$

and capacity ratio in % is calculated from (12).

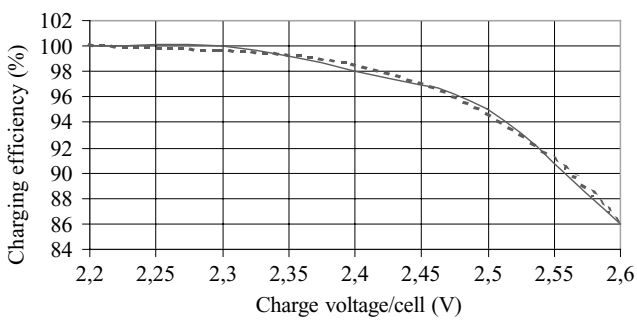

Fig. 4. Charging efficiency at various constant charge voltages.

2.2. SOC estimation during charge

During charge, SOC is monitored by taking into account the charging efficiency during coulometric measurements. Charging efficiency depends on the charge strategy employed. There are two fundamentally different charging methods for lead–acid batteries: constant voltage charge, and constant current charge. In constant voltage charge, voltage across the battery terminals is kept constant, and the condition of the battery determines the charge current. The charging process is usually terminated after a certain time limit is reached, or when charge current falls below a certain limit. Another adopted technique is constant current charge, which automatically equalizes the charge in the series cells. Combination of constant current and constant voltage charge methods are available for lead–acid battery chargers, implemented as the bulk, over, and float charges. In bulk charge, a constant current is applied (typically between $C/5$ and $2C$) to restore the majority of battery capacity. Controlled overcharging follows the bulk charge to restore full capacity in a minimum amount of time. The overcharge voltage depends on the bulk charge rate, and is a constant voltage chosen typically between 2.3 and 2.6 V per cell. Overcharge is terminated when the current reduces to a low value, e.g. one-tenth of bulk charge rate. In float charge, a lower fixed voltage is applied to the battery to maintain full capacity against self-discharge.

Charging efficiency is a function of battery voltage and charge rate. Fig. 4 gives a typical curve of lead–acid cell charging efficiency versus voltage for various constant charge voltages. Increasing voltage decreases the efficiency because of increased parasitic currents [1]. The equation of the curve in Fig. 4 is obtained by curve fitting method, and given in (15), as an expression for constant V_{ch}. The curve of charging efficiency versus constant-current charge rates [1] is given in Fig. 5. At rates up to $C/10$, the efficiency approaches 100%, and decreases at higher rates. The equation of this curve is also given in (15), as an expression for constant charge rate C_R.

$$\eta_{ch} = \begin{cases} -333.3V_{ch}^3 + 2264.3V_{ch}^2 \\ \quad -5130.2V_{ch} + 3976.8; & \text{for constant } V_{ch} \\ -45.1C_R + 100.0; & \text{for constant } C_R \end{cases} \quad (15)$$

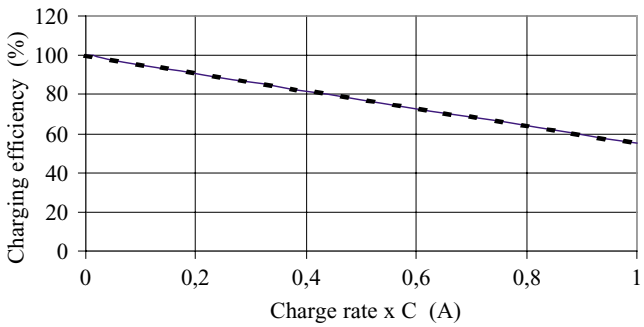

Fig. 5. Charging efficiency vs. constant-current charge rates.

where η_{ch} is the charging efficiency in percent, V_{ch} the charge voltage per cell, and C_R the charge rate.

The effect of temperature is taken into account by using the $k_T(T)$ coefficient calculated by (14). During charge, the current–time product is divided by this coefficient (instead of being multiplied as done during discharge), because the capacity of the battery falls down. As a result, the used capacity can be calculated by

$$C_u(t) = \int_0^t \frac{1}{k_T(T)} \frac{\eta_{ch}}{100} A \, dt \quad (16)$$

where η_{ch} for constant voltage, or constant current charges is calculated from (15).

2.3. Capacity estimation

Many factors, such as overdischarge, discharge current magnitude, charge current magnitude, ageing, etc., can cause a reduction in the available capacity of a lead–acid battery. Capacity estimation can be made when the battery is fully discharged or fully charged. When the battery is fully discharged, the estimated capacity can be calculated by subtracting the calculated remaining capacity during monitoring from the available capacity. The estimated capacity is then used as the new available capacity. In order to use this method, it is necessary to determine when the battery is fully discharged. This can be found from the voltage level of the battery on load. Since the end voltage decreases with increasing discharge current (Fig. 1), Fig. 6 can be adopted to find the relationship between end voltage, and discharge current. A straight-line function is fit to the curve to calculate the end voltage for discharge current rates exceeding 20%. By using (17), the measured battery voltage can be compared with the end voltage to determine the fully discharged state of the battery.

$$V_e = 1.75\left[-0.188\frac{A}{C} + 1.04\right]N \quad (17)$$

where V_e is the end voltage, and N the number of cells.

When the battery is fully charged, the estimated capacity will be equal to the calculated remaining capacity during monitoring. To use this method, it is necessary to determine when the battery is fully charged. Controlled overcharge restores the full capacity of a lead–acid battery. Therefore, the remaining capacity at the transition from overcharge to float charge will give the estimated capacity, which can then be used as the new available capacity.

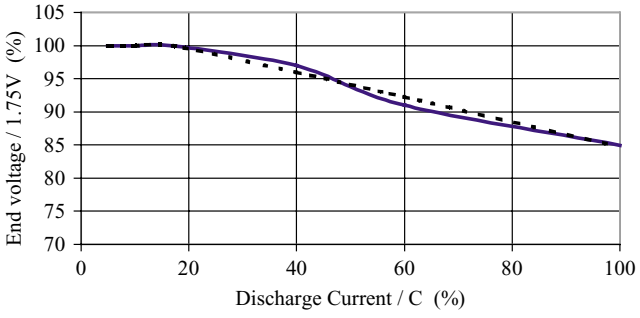

Fig. 6. End voltage vs. discharge current.

3. Implementation

3.1. Hardware implementation

The implementation of the battery monitoring system given in Fig. 7 is based on a low cost 8-bit microcontroller, and its peripherals. The control unit, managing the battery monitoring process, consists of six blocks: the microcontroller (MCU), analog-to-digital converter (A/D), analog interface, display and keyboard, non-volatile memory, and temperature sensor.

The monitoring algorithm is implemented by an 8-bit flash memory microcontroller from NEC, uPD78F0058. In the designed battery monitoring system, the microcontroller uses a 12-bit serial analog-to-digital converter (A/D) from Analog Device (AD7888) for measuring the battery voltage, and current. Analog interface circuit is used to convert the measured battery voltage and current signals to a level which is in the input range of the A/D. The communication between the microcontroller, and A/D is based on synchronous serial communication.

In the implemented system, 100 mV resolution in the range 0–80 V for voltage measurement, and 500 mA resolution in the range −200 to 200 A for current measurements can be obtained. In practice, the current resolution range can be modified according to rated capacity of the battery by changing the gain in the analog interface, e.g. for ±20 A

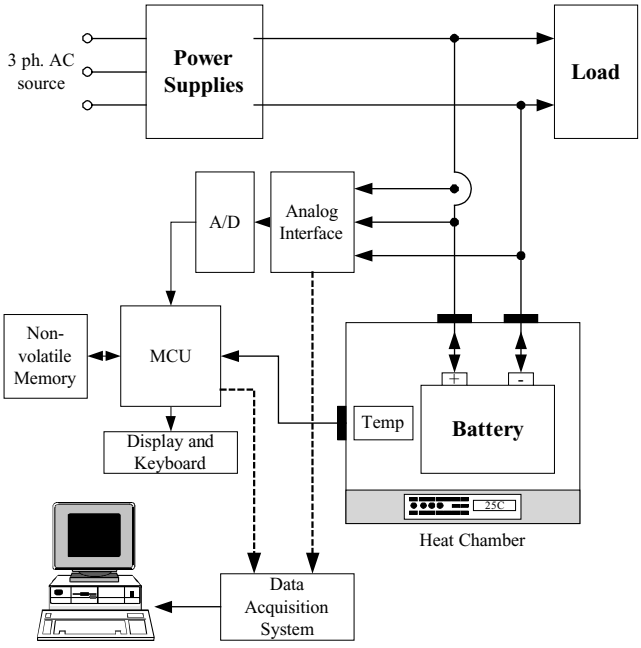

Fig. 7. Hardware block diagram of the monitoring system.

measurement range, it is possible to obtain a resolution of 50 mA.

In the applied algorithm, the ambient temperature is also needed to take into account the effect of temperature on the battery SOC. For this purpose, a temperature module is implemented by a digital thermometer (from Dallas, DS1820). A display and keyboard module is designed to enable the user to input the necessary data and to output the results of the battery monitoring process. To save the data supplied by the user, a non-volatile memory is needed. In the designed system, an EEPROM from XICOR, X1243, is used for this purpose.

3.2. Software implementation

3.2.1. Monitoring during discharge

As mentioned in Section 2, k_{dc} versus discharge current characteristics differ even for battery types from the same manufacturer. Therefore, it is necessary to construct these characteristics from the manufacturer's data. For this purpose, the system demands the current which can be released by battery cells, or blocks at a temperature of 20 °C over 30 min, 1, 3, 5, 8, 10 and 20 h ranges. These data can be obtained easily from the manufacturer's data sheets. The user inputs these data through the display and keyboard available on the system. By using these data and by applying piecewise linearization method, the monitoring system calculates k_{dc} versus discharge current (C) for the given battery, and converts this curve to a look-up table which is used for monitoring during discharge. The system also stores the data given by the user to the EEPROM.

The curve of k_{ev} versus discharge current (C) however is similar for all types of lead–acid batteries. Therefore, coefficient k_{ev} is calculated for each percentage of the discharge current (C), and stored to flash memory. Similarly the curve of k_T versus temperature is also assumed to be the same for all lead–acid battery types. This coefficient is then calculated for a temperature range 0–50 °C with 1 °C resolution, and stored to flash memory. At the beginning of the discharge, capacity rating for 20 h, which is denoted as the available capacity C, is converted to ampere-second, and saved as remaining ampere-second rating. Then, the battery current is read every second and it is divided by the C rating. The coefficients k_{dc} and k_{ev} corresponding to the discharge current percentage are read from the look-up table. The temperature is sensed by the temperature module, and the corresponding k_T is obtained from the look-up table available in memory. In the designed battery monitoring system, k_{dc} is calculated on 120 basis, i.e. 1 corresponds to 120, k_{ev} is calculated on 100 basis, and k_T is calculated on 127 basis. As a result, the remaining capacity is expressed as given in (20).

$$C_r[n] = C_r[n-1] - \left(\frac{k_{dc}[A[n]100/C]}{k_{ev}[A[n]100/C]}A[n]\right)\frac{100}{120}\frac{k_T(T)}{127} \quad (20)$$

where $C_r[n]$ is the remaining capacity at time n, $C_r[0]$ the ampere-second rating corresponding to C rating, n the time in seconds, and $A[n]$ the current at time n.

In the designed system, the remaining percentage of the battery capacity is displayed as calculated by (21).

$$\%C_r[n] = \frac{C_r[n]100}{C} \quad (21)$$

3.2.2. Monitoring during charge

As mentioned in Section 2, to calculate the remaining capacity, charging efficiency coefficient, η_{ch} must be determined. The calculation method differs depending on the charge state. It is clear from the charging efficiency versus voltage curve (Fig. 4), that the charging efficiency is 100% for voltages less than 2.3 V per cell. Therefore, for voltages less than 2.3 V per cell, one can assume a constant-current charge state. When the voltage exceeds this level, the battery current will drop because of lead–acid battery characteristics. It is clear from the charging efficiency versus constant-current charge rate curve (Fig. 5) that at rates up to $C/10$, η_{ch} approaches 100%. By using this fact, for voltages greater than 2.3 V per cell, the charge state can be assumed as constant voltage state. Therefore, coefficient η_{ch} can be calculated by using the expression for constant voltages in (15). For constant voltage charge, Eq. (15) is converted to a look-up table for cell voltages in the range 2.3–2.6 V per cell in 0.01 V resolution, and saved to flash memory of the used microcontroller. For constant current charges, since η_{ch} has a straight-line variation against charge rate, it can then be directly processed by the microcontroller during execution. Furthermore, for SOC estimation during charge, coefficient k_T is also needed. In the discharge part, it has been stated that this coefficient is calculated for a temperature range of 0–50 °C in 1 °C resolution, and stored to flash memory. The remaining capacity during charge mode is then calculated from (22) and (23).

$$C_r[n] = C_r[n-1] + \eta_{ch}\left(\frac{A[n]100}{C}\right)\frac{A[n]}{100}\frac{127}{k_T(T)}, \quad \text{for } V \le 2.3\,\text{V per cell} \quad (22)$$

$$C_r[n] = C_r[n-1] + \eta_{ch}\left(\frac{V[n]100}{N}\right)\frac{A[n]}{100}\frac{127}{k_T(T)}, \quad \text{for } V > 2.3\,\text{V per cell} \quad (23)$$

where N is the number of cells, $V[n]$ the voltage at time n, and $A[n]$ the current at time n.

3.2.3. Capacity estimation

In the designed system, the capacity estimation is made both at the end of each discharge and each charge period. For the discharge period, the end voltage per cell for each discharge current rate is calculated in 1% resolution as defined in Section 2, and saved to flash memory. During discharge, the microcontroller monitors the output voltage, and compares it with the end voltage corresponding to the discharge

current rate. In case the output voltage is less than or equal to the end voltage, microcontroller checks the remaining percentage of the battery capacity. If it is greater than 3%, microcontroller calculates the new capacity C_{new} by using (24). C_{new} is then used as available capacity C after this calculation.

$$C_{new} = C\left(\frac{100 - \%C_r[n]}{100}\right) \quad (24)$$

During charging process, the microcontroller determines the end of charge period by monitoring the battery current. If battery current is less than a preset value, which can be adjusted by using display and keyboard, microcontroller decides that the charge process is completed, and in case the remaining percentage of the battery capacity is less than 97%, it calculates the new capacity by using (25).

$$C_{new} = C\frac{\%C_r[n]}{100} \quad (25)$$

The flowchart of the software implementing the proposed battery monitoring algorithm explained above is given in Fig. 8.

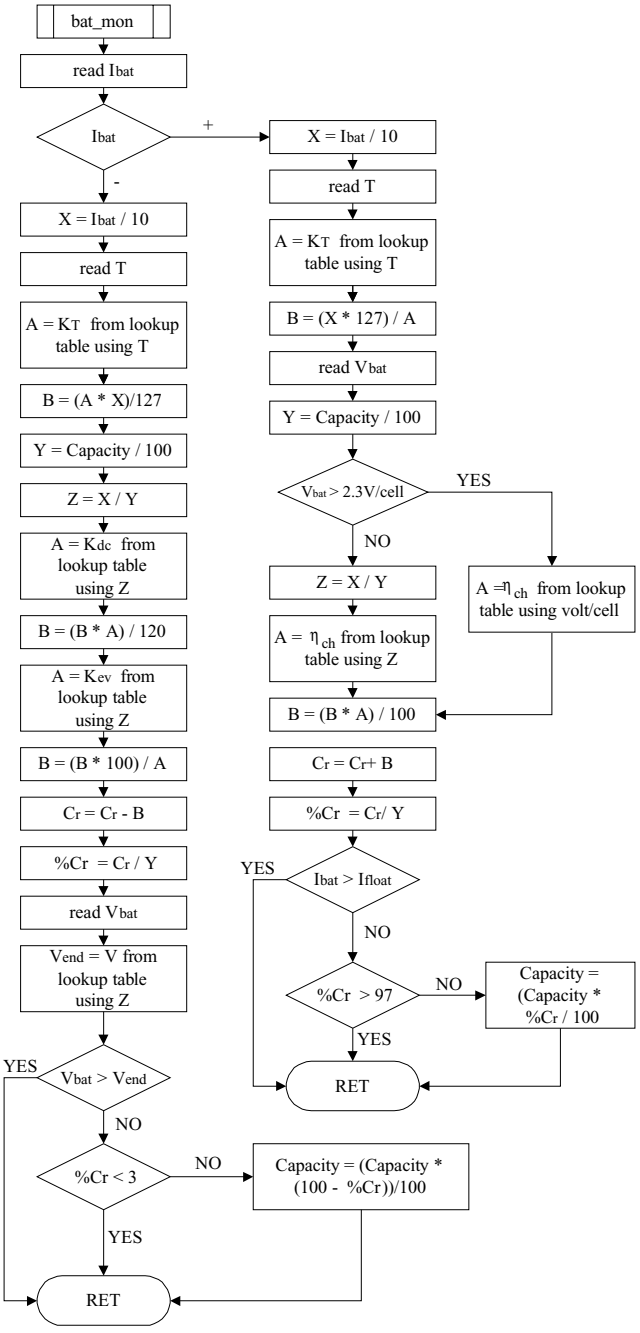

Fig. 8. Flowchart of the battery monitoring algorithm.

4. Experimental results

The validity of the proposed SOC monitoring method is verified by means of a series of experimental tests carried out using the set-up given in Fig. 7. In the test set-up, battery voltage and battery current waveforms are taken from the Hall-effect voltage and current transducers by means of the analog interface. The data are sampled at 5 Hz, and recorded on a PC, using a data acquisition system. The data acquisition system used consists of a LabVIEW software, a data acquisition card (PCI-MIO-16E-1), and a sample and hold card (SC-2040), from National Instruments.

The PCI-MIO-16E-1 converts analog inputs to digital data at 1.25 MS/s rate with 12-bit resolution. It has 16 single ended analog inputs. SC-2040 has eight differential analog inputs, each of which has its own instrumentation amplifier. The microcontroller outputs the calculated SOC of batteries, by using its embedded digital-to-analog converter. Then, SOC is recorded as an analog signal by the data acquisition system. The collected data are processed by MATLAB software, and the time variations of battery voltage, battery current and SOC are obtained for different charge–discharge strategies. To verify the performance of the system at different temperatures, a heat chamber has been employed during tests.

The tests are conducted first on 4 × 12 V, 38 Ah rated capacity Fulmen monoblock valve-regulated, lead–acid batteries, Shc140, and then on some aged batteries of 4-year old, 4 × 12 V, 90 Ah rated capacity, Fulmen Shc290. The manufacturer's data giving the necessary constant currents to be supplied to the tested batteries, to discharge them down to 1.75 V per cell level for different time durations are given in Appendix B. These data are input to the system by means of display and keyboard. The results of the experimental tests are verified by means of open-circuit voltage of a cell, which is considered as an accurate indicator of SOC. Fig. 9 shows the relationship between open-circuit voltage, and remaining capacity of a typical lead–acid cell [1].

4.1. Test 1: battery capacity estimation

In this test, the actual capacity of a 1-year old lead–acid battery block (Shc140, from Fulmen) is determined. The

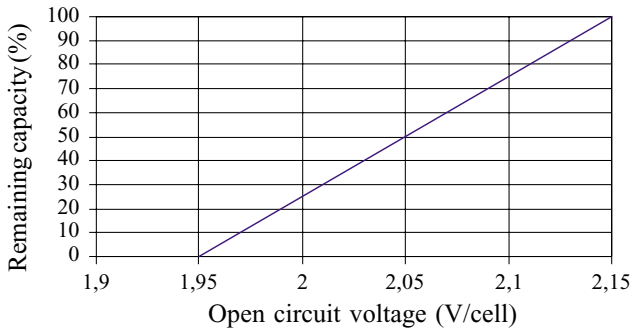

Fig. 9. Open-circuit voltage as indicator of remaining capacity.

rated capacity is input to the system as 38Ah, from the nameplate data of the battery itself. Then, the battery is discharged at a constant current of 5 A, and when its voltage reached the end voltage of 42 V, the monitoring system reported the remaining capacity to be 30% of actual capacity given by the manufacturer. The available capacity of the sample battery block is then calculated as 27 Ah. The corresponding battery voltage, battery current and SOC, recorded during the discharge period by means of the data acquisition system are given in Fig. 10.

4.2. Test 2: monitoring during bulk, over, and float charges

In this test, the same 48 V battery having 27 Ah of available capacity is charged with constant current (bulk charge with *C*/7) until the battery voltage reaches 57.6 V, and then with constant voltage (overcharge with 2.40 V per cell) until the battery current falls below 500 mA, where the float charge begins with 53.5 V (2.23 V per cell) constant voltage applied to the battery. The battery voltage, battery current, and SOC variations against time are sampled during the whole charging period, and monitored as given in Fig. 11. At the end of the constant voltage charging period, the system reported remaining charge as 100%, as expected. The validity of SOC determined by the monitoring system is verified by reading the open-circuit voltage of the battery after a sufficiently long stabilization period.

The open-circuit voltage is measured to be 51.6 V, which corresponds to 2.15 V per cell, indicating that the battery block is fully charged, as verified from the remaining capacity versus open-circuit voltage per cell characteristic given in Fig. 9, as indicator of the actual SOC.

4.3. Test 3: constant-current discharge test

The discharge test is carried out on the same battery at a constant-current discharge rate of 5 A, and at an ambient temperature of 20 °C. The corresponding battery voltage, battery current and SOC profiles are presented in Fig. 12. When the battery is discharged at a 5 A rate its voltage falls down to 42 V in 320 min, and the system reports SOC to be 0%. According to Fig. 1 given in Section 2, for a 5 A discharge, which corresponds to a discharge rate at 18% of available capacity, battery end voltage should be 42 V. Although this typical global voltage value which corresponds to 1.75 V per cell does not reflect the heterogeneity of elements, it is a good approximation for new cells. As seen from Fig. 12, the end voltage is near 42 V. To take into account the heterogeneity of elements, the 'end voltage' can be adjusted by the user from software. Finally, the load is disconnected to verify the estimated SOC by recording the open-circuit voltage. After a sufficiently long recovery time (≈20 h later), the open-circuit voltage is

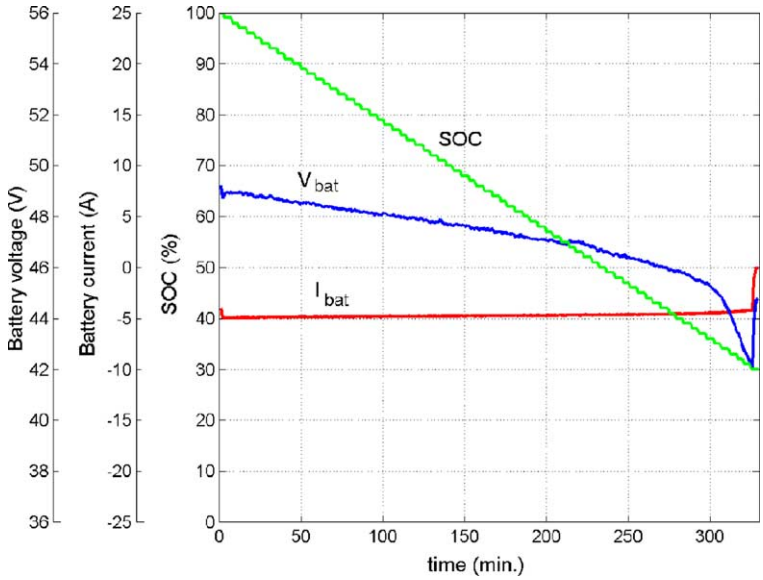

Fig. 10. Battery voltage, battery current, and SOC during capacity estimation (test 1).

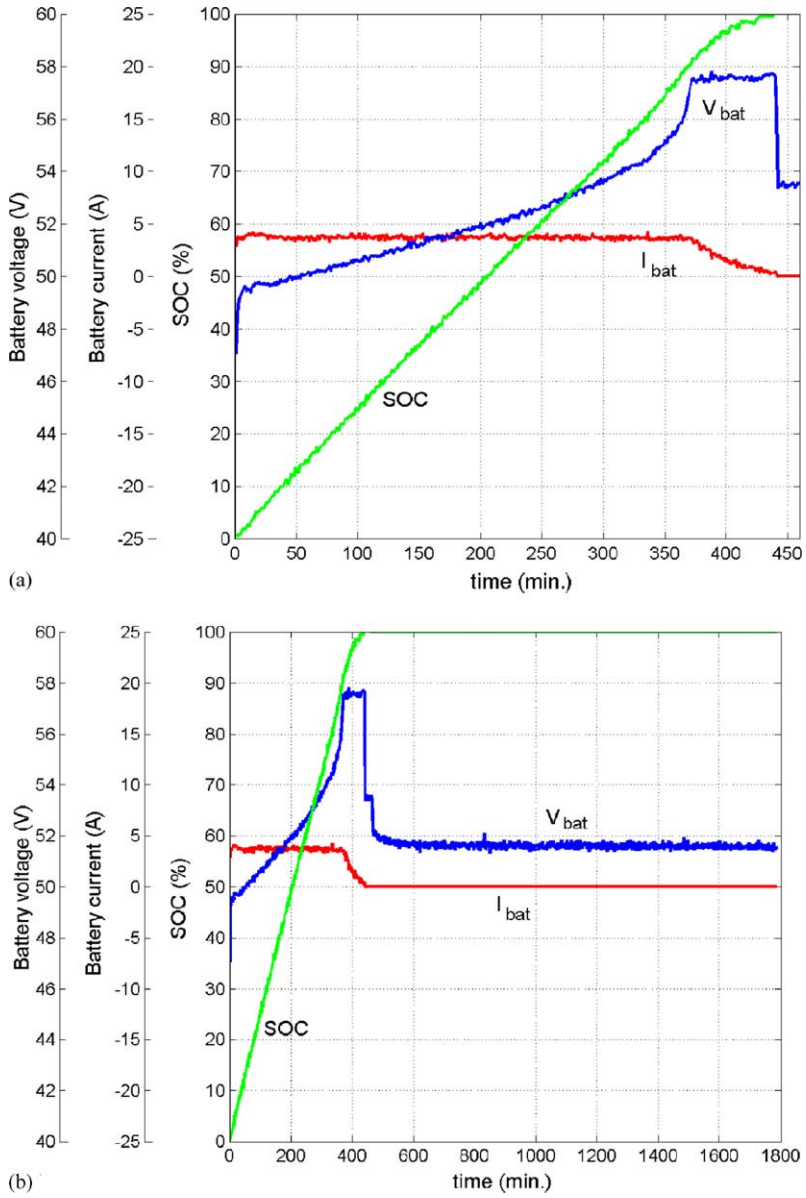

Fig. 11. Battery voltage, battery current, and SOC estimation during charge (test 2): (a) during bulk, over, and float charges; (b) verification of SOC monitoring by open-circuit test after charge.

read to be 46.8 V, which corresponds to 1.95 V per cell, as expected.

4.4. Test 4: variable load discharge

In this test, the battery is discharged with variable current, and the battery voltage, battery current and SOC are monitored as given in Fig. 13. The SOC curve changes its slope according to the discharge current. During the last period of the variable-load discharge test, the battery is discharged with 5 A, and the system reported SOC to be 0% when the output voltage falls to 42 V, as expected. Then, the load is disconnected, and the open-circuit voltage is found out to be 46.8 V, which corresponds to 1.95 V per cell, i.e. to 0% remaining capacity as verified from Fig. 9.

4.5. Test 5: alternate charge–discharge test

In this test, the battery is charged, and discharged sequentially to simulate the occurrence of mains failure soon after being recovered from a previous failure, under variable load condition. During the first 440 min, constant current charge is applied to the battery with intermittent discharge periods, and finally constant voltage charge is applied until the current falls below 750 mA. At this point, the system reported the SOC to be 100% as expected. The corresponding battery voltage, current, and SOC waveforms monitored by the system can be clearly seen from Fig. 14. At the end of the test, the system is held in float mode for a very short time period, and to verify the validity of the monitored SOC, the battery is open circuited. Twenty hours later,

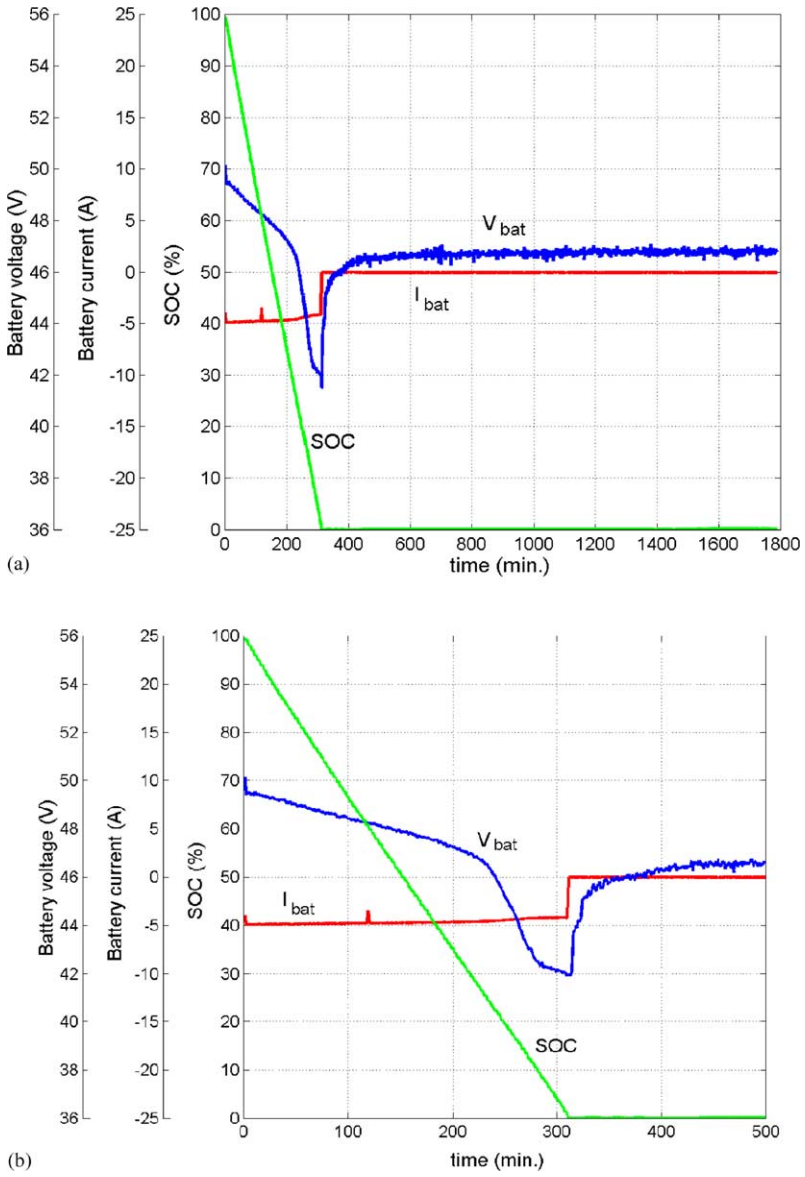

Fig. 12. Battery voltage, battery current, and SOC profiles during constant-current discharge test (test 3): (a) under open-circuit condition after discharge with 5 A; (b) discharge with 5 A.

the open-circuit voltage is measured to be 51.6 V, which corresponds to 2.15 V per cell, as expected.

4.6. Test 6: effects of temperature

In this test, the battery is discharged with 5 A at different ambient temperatures lying between 0 and 45 °C, and the corresponding battery voltage, battery current and SOC variations against time are recorded. SOC profiles against different ambient temperatures between 0 and 45 °C are given in Fig. 15, for a constant discharge rate of 5 A.

4.7. Test 7: monitoring of aged cells

Determination of available capacity by using battery recharacterization, and discharge/charge performance has been obtained as given in Fig. 16, for 4 × 12 V, 4-year old battery blocks from Fulmen, with a rated capacity of 90 Ah (Shc290). A battery block in float state is discharged to the end voltage, and new available capacity is estimated as ≈20% of old available capacity.

It is worth to note that the battery voltage characteristic is distorted in some range at the end of discharge period due to ageing. For aged cells, some elements are in inversed polarity. It is therefore not suitable to make use of battery voltage measurements under load for capacity estimation of aged cells, due to heterogeneity of elements. Available capacity is then corrected as 19 Ah. Hundred percentage of available capacity is indeed reached at the end of the succeeding charge period as seen from monitored SOC in Fig. 16. In the proposed system, the end voltage can be modified by the user, adjusting this parameter from software

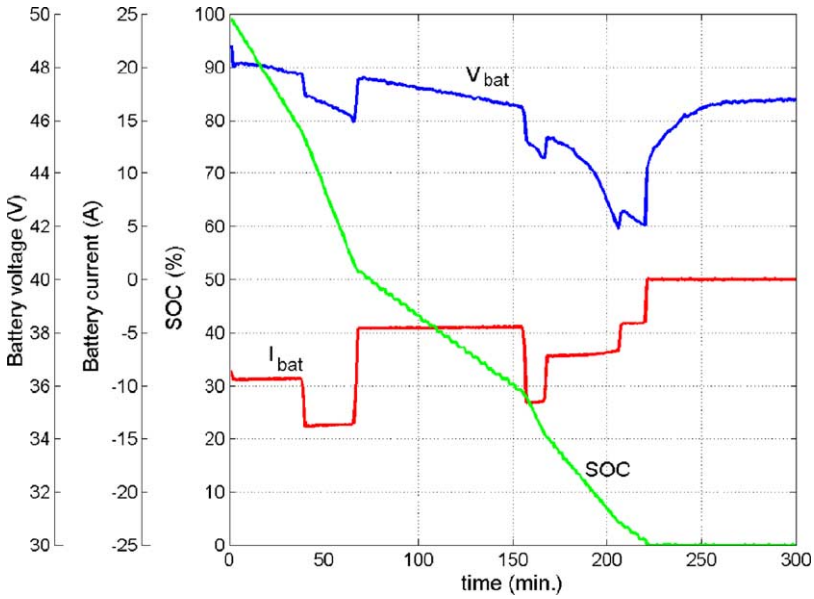

Fig. 13. Battery voltage, battery current, and SOC for variable-load discharge (test 4).

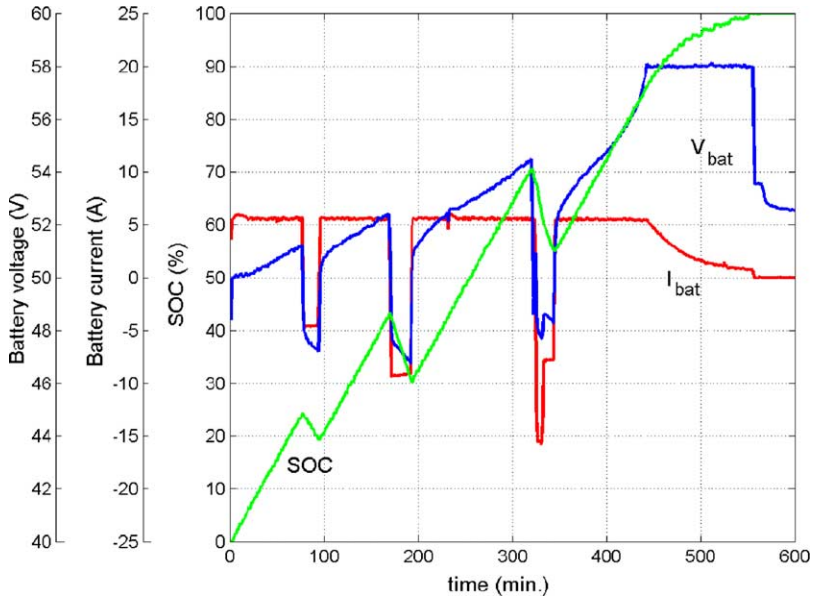

Fig. 14. Battery voltage, battery current, and SOC for alternate charge–discharge (test 5).

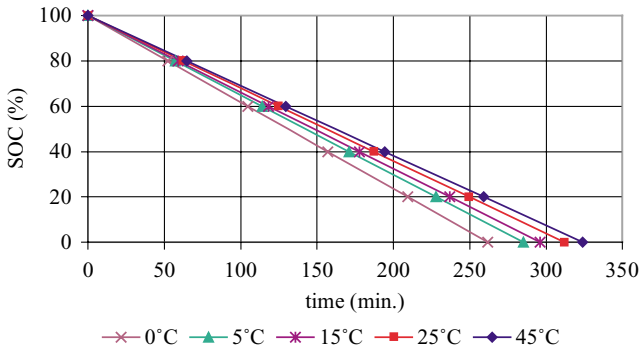

Fig. 15. SOC vs. time at different temperatures.

after recharacterization. A reasonable cut-off voltage should be near 45 V in Fig. 16.

5. Implemented SOC estimation system

The proposed system has been implemented to monitor the SOC of 6 × 90 Ah back-up valve-regulated, lead–acid battery blocks used in a telecommunication power system as shown in Fig. 17. The corresponding battery monitoring menu is as illustrated in Fig. 18. Battery monitoring process can be enabled or disabled by using this menu. The > or < buttons toggle the state of the battery monitoring while this menu is active. The rated capacity shown on this menu rep-

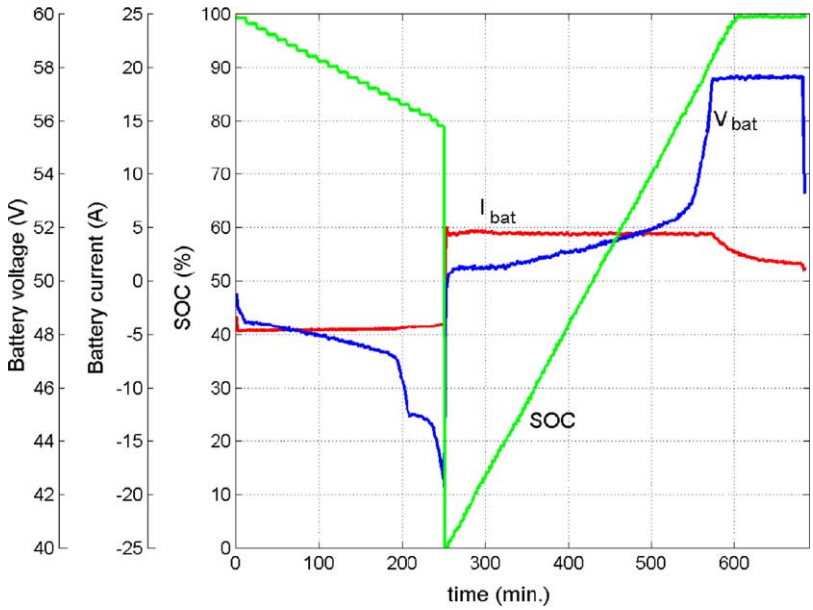

Fig. 16. Recharacterization and discharge/charge performance of aged cells.

resents the nameplate data of the battery, while the available capacity is the representation of the calculated capacity of the battery after recharacterization. As the battery gets aged, the available capacity falls below the rated capacity. The remaining capacity indicates the instantaneous state-of-charge of the battery both in percent, and ampere-hour representations.

On the last line of this menu, the battery voltage and battery current are shown. The negative battery current shows that the battery is feeding the load, while the positive battery current indicates that the battery is being charged.

Fig. 17. Battery monitoring implemented on a telecommunication power system.

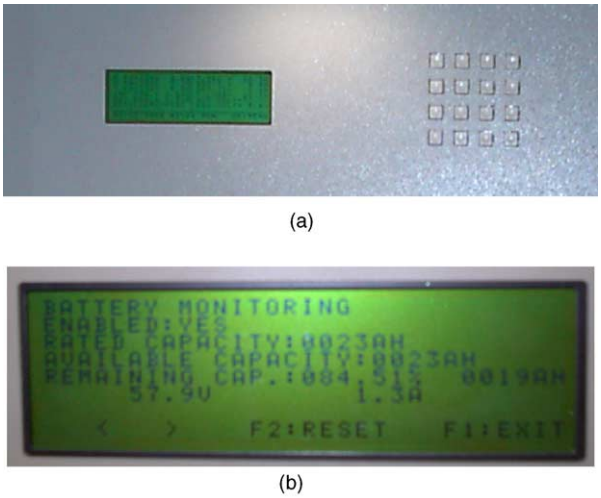

Fig. 18. Monitoring system menu: (a) display and keypad; (b) battery monitoring menu.

6. Conclusions

A new technique has been presented for on-line SOC estimation, and monitoring of sealed lead–acid batteries during both discharge, and charge periods. The proposed technique is based on discharge time versus discharge rate data given in manufacturer's data sheets, combined with coulometric measurements, without the necessity for any open-circuit voltage measurement. Available capacity of the battery is also estimated at the end of each charge, and each discharge period. This technique is successfully implemented, and tested on telecommunication power systems. It is shown to be valid for various operating conditions in practice, including different charge–discharge rates and strategies, variable

load conditions, different ambient temperatures, and aged lead–acid cells. An accuracy in SOC estimation better than 3–4% has been obtained for all operating conditions. Discrepencies between monitored, and theoretical SOCs are due to measurement/resolution errors, and slight differences between manufacturers' characteristics.

The proposed SOC estimator has the advantage of easy implementation by software on a simple 8-bit microcontroller, with minimum hardware requirement. Eventhough the system has been tested specifically on valve-regulated, lead–acid batteries used in telecommunication power supplies, it can be generalized to some other applications employing lead–acid batteries, such as UPS systems, emergency power, solar-photovoltaic systems, electric vehicles, submarine service, etc., with slight modifications in design due to possible changes in battery characteristics, and manufacturers' data.

Appendix A. Coefficients for discharge current vs. discharge current/*C* curves for different lead–acid batteries

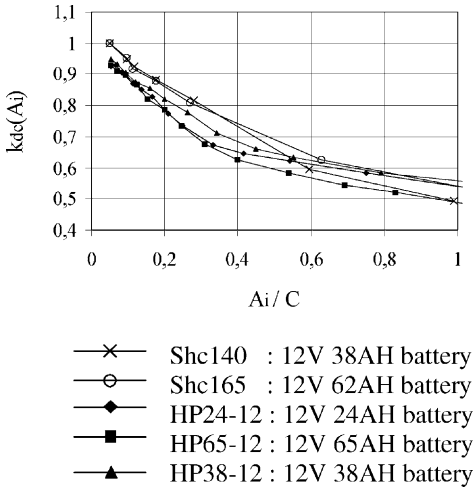

Appendix B. Discharge time versus discharge rate data of tested batteries

Discharge data for Fulmen Shc140 battery blocks from manufacturer's rapid determination tables

Discharge time	Discharge rate (A)
30 min	37.6
1 h	22.6
3 h	10.6
5 h	6.7
8 h	4.4
10 h	3.7
20 h	1.9

End of discharge voltage: 1.75 V; temperature: 20 °C

Discharge data for Fulmen Shc290 battery blocks from manufacturer's rapid determination tables

Discharge time	Discharge rate (A)
30 min	80.8
1 h	50.2
3 h	22.3
5 h	14.7
8 h	10.0
10 h	8.6
20 h	4.5

End of discharge voltage: 1.75 V; temperature: 20 °C

References

[1] D. Linden, Handbook of Batteries, McGraw-Hill, New York, 1995.
[2] J.P. Cun, J.N. Fiorina, M. Fraisse, H. Mabboux, The experience of a UPS company in advanced battery monitoring, Intelec'96, Boston, US, 1996, pp. 22–25.
[3] I. Kurisawa, M. Iwata, Internal resistance and deterioration of VRLA battery—analysis of internal resistance obtained by direct current measurement and its application to VRLA battery monitoring technique', Intelec'97, Melbourne, Australia, 1997, pp. 29–33.
[4] R.V. Biagetti, A.M. Pesco, Apparatus and method for adaptively predicting battery discharge reserve time, US Patent 4 952 862 (1989).
[5] T. Hubert, A battery system using adaptive run-time estimation, software controlled multi-mode charging and intrinsic diagnostics combined to enhance UPS reliability', in: Proceedings of the HFPC'95, pp. 382–395.
[6] M.A. Casacca, Z.M. Salameh, Determination of lead–acid battery capacity via mathematical modeling techniques, IEEE Trans. Energy Conv. 7 (3) (1992) 442–446.
[7] A.H. Anbuky, P.E. Pascoe, VRLA battery state of charge estimation in telecommunication power systems, IEEE Trans. Ind. Electron. 47 (3) (2000) 565–573.
[8] M. Kozaki, T. Yamazaki, Remaining battery capacity meter and method for computing remaining capacity, US Patent 5 691 078 (1997).
[9] J.H. Aylor, A. Thieme, B.W. Johnson, A battery state-of-charge indicator for electric wheelchairs, IEEE Trans. Ind. Electron. 39 (5) (1992) 398–409.
[10] S. Piller, M. Perrin, A. Jossen, Methods for state of charge determination and their applications, J. Power Sour. 96 (1) (2001) 113–120.
[11] I.R. Hill, E.E. Andrukaitis, Non-intrusive measurement of the state-of-charge of lead–acid batteries using wire-wound coils, J. Power Sour. 103 (1) (2001) 98–112.
[12] J.D. Weiss, B.R. Stallard, M.J. Garcia, Using optical absorption to measure state of charge of lead acid batteries, Opt. Eng. 37 (12) (1998) 3254–3259.